Proceedings of the International Association for Shell and Spatial Structures (IASS) Symposium 2009, Valencia
Evolution and Trends in Design, Analysis and Construction of Shell and Spatial Structures
28 September - 2 October 2009, Universidad Politécnica de Valencia, Spain
Alberto DOMINGO and Carlos LAZARO (eds.)

A large displacement structural analysis of a pipeline subjected to gravity and buoyancy forces

Juan Carlos Mosquera*, Jaime García-Palacios[a] and Avelino Samartín[b]

* Assistant Professor. Dept. of Structural Mechanics
ETSICCYP. UPM. Ciudad Universitaria s/n. 28040 Madrid
juancarlos.mosquera@upm.es

[a] Assistant Professor. of Civil Engineering: Hydraulic and Energetic, UPM. Madrid
[b] Full Professor. Dept. of Structural Mechanics, UPM. Madrid

Abstract

A nonlinear analysis of an elastic tube subjected to gravity forces and buoyancy pressure is carried out. An update lagrangian formulation is used. The structural analysis efficiency in terms of computer time and accuracy, has been improved when load stiffness matrices have been introduced. In this way the follower forces characteristics such as their intensity and direction changes can be well represented. A sensitivity study of different involved variables on the final deformed pipeline shape is carried out.

Keywords: Geometrically nonlinear structures, large displacements, follower forces, hydrostatic actions

1. Introduction

It is considered a pipeline of total length $L_T = NL$. For analysis purpose the pipeline is divided into N segments of equal length L. Each element i with $i = 1, 2, \ldots, N$ is limited by two nodes, 1 and 2, using local numbering and $n - 1$ e n in global numbering in which n varies from 0 to N. The two extreme nodes 0 and N correspond to two lids of weight $P_{L\alpha}$, with $\alpha = 0$ and $\alpha = 1$ as it is shown in figure 1a.

The circular constant section of the pipeline has an external radius R. The weight of the tube is represented by a uniform distributed load of intensity p per unit of length. In addition, the tube is floating on the sea and therefore it is subjected to an upward hydrostatic pressure. The sea density is γ_w. Waves and current forces does not exist. Therefore, it is assumed inertia forces are negligible. The tube elasto-mechanics characteristics are: Young

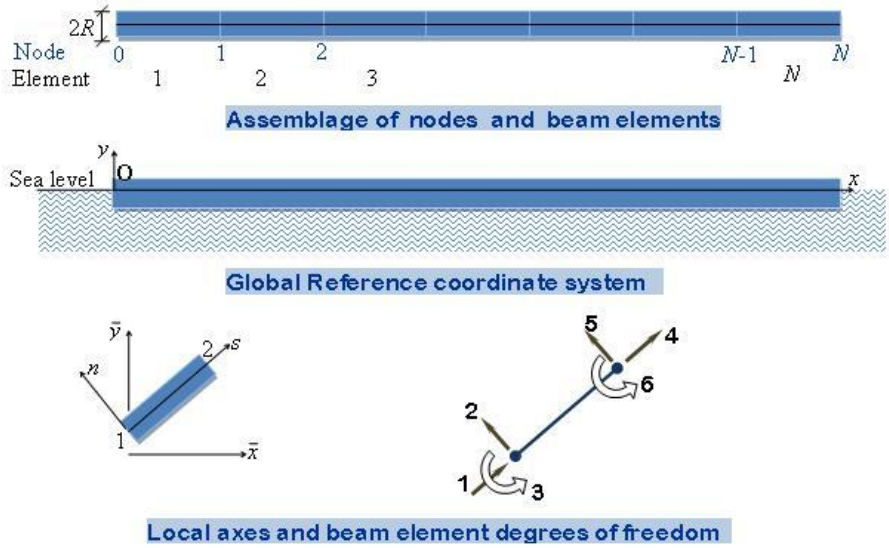

Figure 1: Pipeline discretización

modulus E, flexural inertia I_z and area Ω. All loads are modeled in a first approximation as concentrated at extreme nodes of each pipeline segment.

The objective of this paper is to find the final equilibrated deformed position of the pipeline subjected to the former loads.

The following system of coordinate axes is adopted: General axes Oxy for load definition, in which the origin O s the intersection of the vertical at initial pipeline section and the horizontal corresponding to the still water level (SWL). The axis Ox is horizontal and the axis Oy is upwards vertical (figure 1b). Ii is assumed that inertial forces due to the waves and sea current does not exist. Finally, a local coordinate system s, n is introduced to define the stress-resultants for each pipeline element 12. The origin of these local axes is at node 1 and the axis s is the straight line joining the node 1 and 2. The axis n is normal to the axis s. The axes s, n rotated in such a way that their directions became parallel to horizontal and vertical, i.e. to the general axes Oxy are designated by $\bar{x}, \bar{y}$.

The stress-resultant and displacement analysis will be carried out within a geometrically nonlinear elastic in large displacements framework and an updated Lagrangian formulation. Standard notation will be used in the nonlinear analysis of the structures [3]. The occurrence od a variable in the configuration C_1, $i = 1, 2$, will be designated by a superscript i to the left. The axes of reference of the occurrence of a variable are defined by a left subscript. The subscripts and superscript to the right have either the usual meaning of components of a matrix or a vector or they are used to distinguish the element and section dependence of similar matrices and vectors. The initial position of equilibrium of the tube is achieved assuming that the loads, self weight and hydrostatic pressure on the pipeline caps are null and

therefore only the distributed loading is acting, i.e. the pipeline weight and the Archimedes uplift pressure. In figure 2 the horizontal position of equilibrium of the pipeline is shown. The tube is subjected in this position to its weight balanced by the Archimedes uplift. The remaining loads, the lids weight and the hydrostatic pressure on them, are multiplied by a factor $\lambda = 0$ i.e. they are not acting on the pipeline yet. From this initial position of equilibrium the loading on the extreme sections of the pipeline are increasing continuously by varying the factor λ from its initial value $\lambda = 0$ to the final one $\lambda = 1$. An incremental analysis technique is used starting at current configuration of equilibrium C_1 of the deformed tube, that it corresponds to a value $0 < \lambda < 1$. From this position the lids forces are increasing by the factor $\lambda + d\lambda$ and it is attempting to find the new target configuration of equilibrium C_2 corresponding to these incremental loads. It should be noted that the weight of the pipeline remains constant, both in intensity as in direction, along the length of the tube. Moreover, the Archimedes pressure along the pipeline is not affected by this factor increment $d\lambda$, but due to its follower characteristic attached to the structure, according the classification given in [2], its intensity and direction vary because they are dependent of the deformed geometry of the pipeline. These follower loads not only change its direction due to the incremental rotations occurring at the tube sections along the pipeline, but also its intensity caused by the incremental displacements produced along the pipeline.

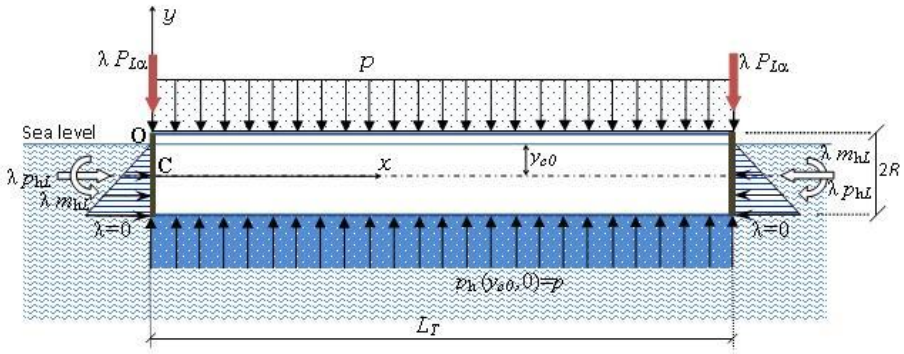

Figure 2: Initial configuración C_0 of the tube in equilibrium

This paper is structured as follows. First, it is studied the hydrostatic pressure on a pipeline slice and its incremental changes when the slice undergoes a differential rotation $d\theta$ and a differential displacement dv_0. Next, for a pipeline element the incremental equilibrium equations between the configurations C_1 and C_2 are set up by applying the principle of virtual work. All variables involved in these equilibrium equations are expressed in axes of the known configuration C_1. In this way the equivalent loads at element nodes are obtained and the stiffness and load matrices are computed as well. The load matrices are caused by the follower forces, i.e. loads whose intensity and direction are depending on element displacements. Once the FE discretization of the whole pipeline has been performed the linearized incremental equilibrium equations can be found. The equilibrium equations can be solved

iteratively until a final equilibrium position at the end of step load $\lambda + d\lambda$ is reached. In these equations the appearance of load stiffness matrices due to the follower loads. By an incremental procedure or a step by step technique the final equilibrium position of the pipeline, i.e. the pipeline position corresponding to the final value of the load factor $\lambda = 1$ can be found. It was found that the inclusion in the analysis of these load matrices allows greater computational efficiency and a better accuracy in the results. Several application examples are shown and in some of them a sensitivity analysis of some key variables illustrate the computational techniques developed. Finally the paper is closed with some general conclusions.

2. Distribution and resultant of the pressure loading on a tube slice

It is assumed a pipeline slice inclined respect to horizontal an angle θ. In figure 3 the hydrostatic pressure distribution on a semi-submerged cross-section of the pipeline is shown. This pressure $p(y_c, \theta, \varphi)$ is function of following variables: the ordinate y_c of the center of the circle, the slope θ of the section respect to the vertical plane and the position of the application point of the pressure defined by the angle φ. The resultant force, $p_h(y_c, \theta)ds$, of this pressure distribution on a pipeline slice of thickness ds is contained in its middle plane.

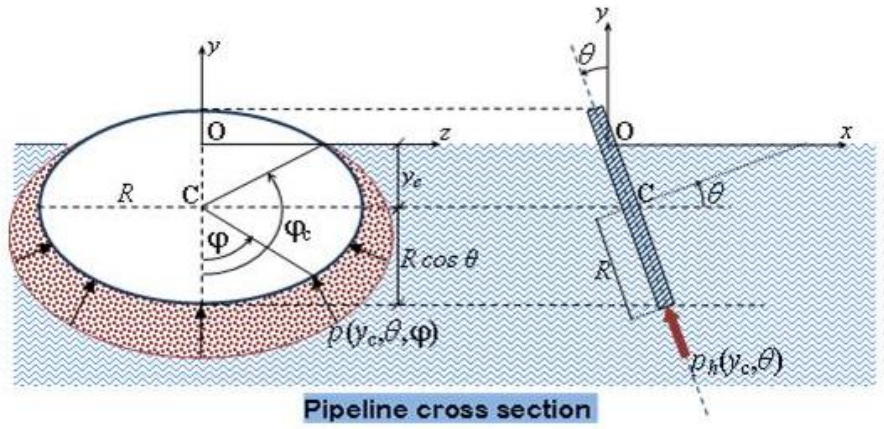

Figure 3: Pressure distribution on a circular section

In the following the expressions of the pressure distribution $p(y_c, \theta, \varphi)$ and its resultant $p_h(y_c, \theta)ds$ as function of the position of the tube center measured by the ordinate y_c are given:

- Slice in the air $y_c \geq R\cos\theta$

$$p(y_c,\theta,\varphi) = 0 \tag{1}$$
$$p_h(y_c,\theta) = 0 \tag{2}$$

- Semi-submerged slice $R\cos\theta \geq y_c \geq -R\cos\theta$

$$p(y_c,\theta,\varphi) = \gamma_w\left[R\cos\theta\cos\varphi - y_c\right] \tag{3}$$
$$\text{with} \quad \varphi_c \geq \varphi \geq -\varphi_c \text{ and } \varphi_c = \arctan\left(\frac{y_c}{R\cos\theta}\right)$$
$$p_h(y_c,\theta) = 2\int_0^{\varphi_c} p(y_c,\theta,\varphi)\cos\varphi R d\varphi =$$
$$\gamma_w R^2\left[\arccos\left(\frac{y_c}{R\cos\theta}\right) - \frac{y_c}{R\cos\theta}\sqrt{1-\left(\frac{y_c}{R\cos\theta}\right)^2}\right] \tag{4}$$

- Submerged slice $-R\cos\theta \geq y_c$

$$p(y_c,\theta,\varphi) = \gamma_w\left(R\cos\theta\cos\varphi - y_c\right) \quad \text{with} \quad -\pi \geq \varphi \geq \pi \tag{5}$$
$$p_h(y_c,\theta) = 2\int_0^{\pi} p(y_c,\theta,\varphi)\cos\varphi R d\varphi = \gamma_w \pi R^2\cos^2\theta \tag{6}$$

The variation of the pressure resultant caused by a modification of the position of the gravity center of the slice defined by an infinitesimal vertical displacement v_0 and an infinitesimal rotation θ_0 are found by the expression:

$$dp_t(y_c,\theta) = \frac{\partial p_h(y_c,\theta)}{\partial y_c}v_0 + \frac{\partial p_h(y_c,\theta)}{\partial\theta}\theta_0$$

in which $\frac{\partial p_h(y_c,\theta)}{\partial y_c}$ and $\frac{\partial p_h(y_c,\theta)}{\partial\theta}$ are defined according to the pipeline slice position as fol-

lows:

Slice in the air $y_c \geq R\cos\theta$

$$\frac{\partial p_h(y_c,\theta)}{\partial y_c} = 0 \tag{7}$$

$$\frac{\partial p_h(y_c,\theta)}{\partial \theta} = 0 \tag{8}$$

Semi-submerged slice $R\cos\theta \geq y_c \geq -R\cos\theta$

$$\frac{\partial p_h(y_c,\theta)}{\partial y_c} = -2\gamma_w R\cos\theta\sqrt{1-\left(\frac{y_c}{R\cos\theta}\right)^2} \tag{9}$$

$$\frac{\partial p_h(y_c,\theta)}{\partial \theta} = -2\gamma_w R^2\cos\theta\sin\theta\arccos\left(\frac{y_c}{R\cos\theta}\right) \tag{10}$$

Submerged slice$-R\cos\theta \geq y_c$

$$\frac{\partial p_h(y_c,\theta)}{\partial y_c} = 0 \tag{11}$$

$$\frac{\partial p_h(y_c,\theta)}{\partial \theta} = -2\gamma_w \pi R^2\cos\theta\sin\theta \tag{12}$$

3. Equivalent loads at element nodes

3..1. Analysis procedure

The analysis of the pipeline structure is carried out according to an incremental procedure, eventually iterative within load steps. That means, the final position of the pipeline is reached by successive finite increments of the load $d\lambda$, starting at the value $\lambda = 0$ and increasing until the final load value $\lambda = 1$. The analysis is described according to an updated lagrangian formulation (UL), in which in each load step the equilibrate configuration C_1 is known and the adopted local coordinate axis for reference **s** and **n** are attached to the known configuration C_1 as it is shown in figure 4. The axis **s** joints nodes 1 and 2 of element and the normal axis **n** corresponds to an anticlockwise rotation of $\frac{\pi}{2}$ of the axis **s**.

3..2. Displacement independent loads

The load of this type acting on the pipeline is the weight and it is assumed this constant load is applied to a beam element of length L inclined an angle α respect to horizontal. The equivalent nodal forces to the weight loading are $\mathbf{p} = (p_{x1}, p_{y1}, m_{z1}, p_{x2}, p_{y2}, m_{z2})^T$ at nodes 1 and 2 and they can be approximately expressed in axes $\bar{x}, \bar{y}$ by means of this formulae:

$$p_{xi} = p_{ti}\cos\alpha - p_{ni}\sin\alpha = 0 \quad i = 1,2 \tag{13}$$

$$p_{yi} = p_{ti}\sin\alpha + p_{ni}\cos\alpha = \frac{pL}{2} \quad i = 1,2 \tag{14}$$

$$m_{zi} = m_{ni} \quad i = 1,2 \tag{15}$$

in which

$$p_{ti} = \int_0^L N_i^1 p ds, \quad i = 1, 2 \tag{16}$$

$$p_{n1} = \int_0^L N_1^3 p ds, \quad m_{n1} = \int_0^L N_2^3 p ds \tag{17}$$

$$p_{n2} = \int_0^L N_3^3 p ds, \quad m_{n2} = \int_0^L N_4^3 p ds \tag{18}$$

In the former expressions the interpolation linear functions have been designed by $N_i^1 = N_i^1(s)$ with $i = 1, 2$ and $N_i^3 = N_i^3(s)$ with $i = 1, 2, 3, 4$ are the cubic interpolation functions of Hermite. They are defined by the expressions:

$$N_1^1 = 1 - \xi, \qquad N_2^1 = \xi \tag{19}$$

$$N_1^3 = 1 - 3\xi^2 + 2\xi^3, \qquad N_3^3 = 3\xi^2 - 2\xi^3 \tag{20}$$

$$N_2^3 = {}^1L\xi(1-\xi)^2, \qquad N_4^3 = {}^1L(\xi^3 - \xi^2) \tag{21}$$

with $\xi = \dfrac{s}{{}^1L}$.

The formulae (16)-(18) are valid only in a linear analysis, however their use in a nonlinear analysis can be acceptable if the beam element length L is small in comparison to the total pipeline length. In the contrary case, the distributed loading on the beam element should be taken into account in the expression of the nonlinear stiffness matrix of the element. Then the expression (72) of this matrix, given later, should be modified and to include terms related to the the distributed force p.

3..3. Follower forces

In the case of follower forces the deformed structure should be taken into account in the analysis. This fact leads to the concept of load stiffness matrix. To this end it is assumed, according to an updated lagrangian formulation, that the equilibrated configuration is known C_1. From this known configuration it is arrived to configuration C_2 when unknown displacements $u(s)$, $v(s)$ and $\theta(s)$ are produced due to a load increment. These displacements are expressed in the local coordinates of the element $\mathbf{s}$ and $\mathbf{n}$.

The geometry of the deformed tube element in the configuration C_1 referred to the local exes can be written if the rotations ${}^1\theta_1$ and ${}^1\theta_2$ at nodes 1 and 2 are known, as follows:

$${}^1y_n(\xi) = N_2^3(\xi){}^1\theta_1 + N_4^3(\xi){}^1\theta_2 \quad \text{with} \quad \xi = \frac{s}{{}^1L} \tag{22}$$

where ${}^1L = \sqrt{({}^1x_2 - {}^1x_1)^2 + ({}^1y_2 - {}^1y_1)^2}$.

The rotation variation along the deformed beam element is

$${}^1\theta_n(\xi) = \frac{d^1y_n(\xi)}{ds} = \frac{dN_2^3(\xi)}{ds}{}^1\theta_1 + \frac{dN_4^3(\xi)}{ds}{}^1\theta_2 \tag{23}$$

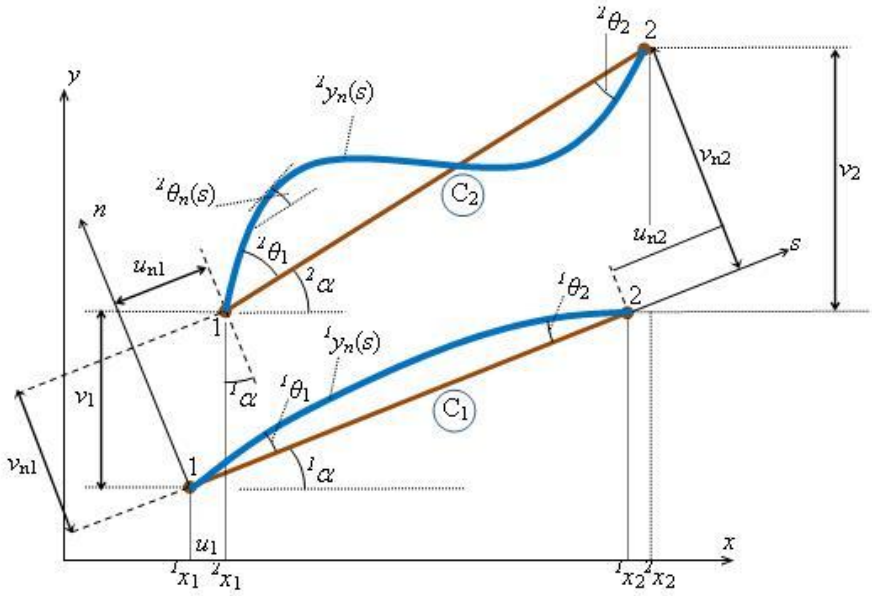

Figure 4: Large displacements in a beam element

If $({}^1x_i, {}^1y_i)$, with $i = 1, 2$, are the general coordinates of the element nodes then the deformed element C_1 in referred to the general axes is:

$$ {}^1y(\xi) = {}^1y_1 + {}^1L\xi \sin {}^1\alpha + {}^1y_n(\xi) \cos {}^1\alpha, \quad {}^1\theta(\xi) = {}^1\theta_n(\xi) + {}^1\alpha \tag{24} $$

with ${}^1\alpha = \arctan({}^1y_2 - {}^1y_1)({}^1x_2 - {}^1x_1)^{-1}$.

The resultant pressure ${}^1p_h(\xi)$ on the slice ξ, noting $y_c(\xi) = y_(\xi)$, can be expressed according to section 2.:

$$ {}^1p_h(\xi) = {}^1p_h[{}^1y_c(\xi), {}^1\theta(\xi)] = {}^1p_h[{}^1y(\xi), {}^1\theta(\xi)] \tag{25} $$

and the local components of this pressure referred to axes **s** and **n** are

$$ {}^1p_{hs}(\xi) = -{}^1p_h(\xi) \sin {}^1\theta \quad \text{and} \quad {}^1p_{hn}(\xi) = {}^1p_h(\xi) \cos {}^1\theta \tag{26} $$

The displacements $u_n(\xi)$, $v_n(\xi)$ and $\theta_n(\xi)$ of the former slice leads this slice from the configuration C_1 to the configuration C_2. These displacements expressed in local axes **s** and **n**

are:

$$u_n(\xi) = \sum_{i=1,2} u_{ni} N_i^1(\xi) \tag{27}$$

$$v_n(\xi) = \sum_{i=1,3} v_{ni} N_i^3(\xi) + \sum_{i=2,4} \theta_{ni} N_i^3(\xi) \tag{28}$$

$$\theta_n(\xi) = \sum_{i=1,3} v_{ni} \frac{dN_i^3(\xi)}{ds} + \sum_{i=2,4} \theta_{ni} \frac{dN_i^3(\xi)}{ds} \tag{29}$$

where u_{ni}, v_{ni} and θ_{ni} are the unknown displacements of node i referred to the element local axes in configuration C^1.

The equations of the deformed tube element in the configuration C_2 expressed in local coordinates, **s** and **n**, are:

$${}^2x_n(\xi) = u_n(\xi), \quad {}^2y_n(\xi) = {}^1y_n + v_n(\xi), \quad \text{and} \quad {}^2\theta_n(\xi) = {}^1\theta_n(\xi) + \theta_n(\xi) \tag{30}$$

which referred to the general axes became:

$${}^2x(\xi) = {}^1x(\xi) + u_n(\xi)\cos{}^1\alpha - {}^1v_n(\xi)\sin{}^1\alpha = {}^1x(\xi) + u(\xi) \tag{31}$$

$${}^2y(\xi) = {}^1y(\xi) + u_n(\xi)\sin{}^1\alpha + {}^1v_n(\xi)\cos{}^1\alpha = {}^1y(\xi) + v(\xi) \tag{32}$$

$${}^2\theta(\xi) = {}^1\theta(\xi) + \theta_n(\xi) \tag{33}$$

The hydrostatic pressure resultant ${}^2p_h(\xi)$ on the slice ξ in the configuration C_2 is now modified to the following value:

$${}^2p_h(\xi) = {}^1p_h[{}^2x(\xi), {}^2y(\xi), {}^2\theta(\xi)] = {}^1p_h[{}^2\mathbf{x}(\xi)] \tag{34}$$

with $\mathbf{x}(\xi) = [{}^2x(\xi), {}^2y(\xi), {}^2\theta(\xi)]$. These pressure components ${}^2p_{hs}(\xi)$ and ${}^2p_{hn}(\xi)$ referred to local axes **s** and **n** are respectively:

$$\begin{aligned} {}^2p_{hs}(\xi) &= -{}^1p_h[{}^2x(\xi), {}^2y(\xi), {}^2\theta(\xi)]\sin{}^2\theta_n(\xi) \\ &= -{}^1p_h[{}^2\mathbf{x}(\xi)]\sin[{}^1\theta_n(\xi) + \theta_n(\xi)] \end{aligned} \tag{35}$$

$$\begin{aligned} {}^2p_{hn}(\xi) &= {}^1p_h[{}^2x(\xi), {}^2y(\xi), {}^2\theta(\xi)]\cos{}^2\theta_n(\xi) \\ &= -{}^1p_h[{}^2\mathbf{x}(\xi)]\cos[{}^1\theta_n(\xi) + \theta_n(\xi)] \end{aligned} \tag{36}$$

In order to find the resultant pressure, $p_h(\xi)$, variation in the slice ξ produced when the slice changes from configuration C_1 to C_2 is necessary to compute the difference ${}^2p_h(\xi) - {}^1p_h(\xi)$. This difference can be expressed in a Taylor expansion in the neighborhood ${}^1p_h(\xi)$. Taking into account (31), (32) and (33) the following expression is obtained:

$${}^2p_h[{}^2\mathbf{x}(\xi)] = {}^1p_h[{}^1\mathbf{x}(\xi)] + A(\xi)\frac{\partial^1 p_h}{\partial y_c} + B(\xi)\frac{\partial^1 p_h}{\partial \theta} \tag{37}$$

where

$$A(\xi) = \sin {}^1\alpha \sum_{i=1,2} u_{ni} N_i^1(\xi) + \cos {}^1\alpha \left(\sum_{i=1,2} v_{ni} N_{2i-1}^3(\xi) + \sum_{i=1,2} \theta_{ni} N_{2i}^3(\xi) \right)$$

$$B(\xi) = \sum_{i=1,2} v_{ni} \frac{dN_{2i-1}^3(\xi)}{d\xi} + \sum_{i=1,2} \theta_{ni} \frac{dN_{2i}^3(\xi)}{d\xi}$$

and therefore resultant pressure components in local exes are:

$$\begin{aligned} {}^2p_{hs}(\xi) &= -{}^1p_h[{}^2\mathbf{x}(\xi)] \sin({}^1\theta_n + \theta_n) = -{}^1p_h[{}^2\mathbf{x}(\xi)] \sin {}^1\theta_n - {}^1p_h[{}^2\mathbf{x}(\xi)]\theta_n \cos {}^1\theta_n \\ &= {}^1p_{hs}[{}^1\mathbf{x}(\xi)] - \sin {}^1\theta_n \left[A(\xi) \frac{\partial^1 p_h}{\partial y_c} + B(\xi) \frac{\partial^1 p_h}{\partial \theta} \right] - {}^1p_{hn}[{}^1\mathbf{x}(\xi)] B(\xi) \\ {}^2p_{hn}(\xi) &= {}^1p_h[{}^2\mathbf{x}(\xi)] \cos({}^1\theta_n + \theta_n) = {}^1p_h[{}^2\mathbf{x}(\xi)] \cos {}^1\theta_n - {}^1p_h[{}^2\mathbf{x}(\xi)]\theta_n \sin {}^1\theta_n \\ &= {}^1p_{hn}[{}^1\mathbf{x}(\xi)] + \cos {}^1\theta_n \left[A(\xi) \frac{\partial^1 p_h}{\partial y_c} + B(\xi) \frac{\partial^1 p_h}{\partial \theta} \right] + {}^1p_{hs}[{}^1\mathbf{x}(\xi)] B(\xi) \end{aligned}$$

The load increments ${}^2p_h(\xi) - {}^1p_h(\xi)$ caused by the element displacement from configuration C_1 to C_2 are substituted by the following equivalent nodal forces $\mathbf{p} = (p_{hsi}, p_{hni}, p_{hmi})$ at element nodes $i = 1, 2$, according to the following expressions in local axes:

$$p_{hsi} = {}^1L \int_0^1 N_i^1 \left[{}^2p_{hs} - {}^1p_{hs} \right] d\xi \quad \text{with} \quad i = 1, 2 \tag{38}$$

$$p_{hn1} = {}^1L \int_0^1 N_1^3 \left[{}^2p_{hn} - {}^1p_{hn} \right] d\xi, \quad p_{hm1} = {}^1L \int_0^1 N_2^3 \left[{}^2p_{hn} - {}^1p_{hn} \right] d\xi \tag{39}$$

$$p_{hn2} = {}^1L \int_0^1 N_3^3 \left[{}^2p_{hn} - {}^1p_{hn} \right] d\xi, \quad p_{hm2} = {}^1L \int_0^1 N_4^3 \left[{}^2p_{hn} - {}^1p_{hn} \right] d\xi \tag{40}$$

3..4. Load stiffness matrices

The follower forces produce equivalent nodal forces that can be represented as stiffness matrices. In the following the variation of the follower forces from configuration C_1 to C_2 is expressed in this more convenient way. With this purpose the functions $A(\xi)$ and $B(\xi)$ are written in matrix form

$$A(\xi) = \mathbf{a}(\xi)\mathbf{d}_n, \quad B(\xi) = \mathbf{b}(\xi)\mathbf{d}_n \tag{41}$$

where $\mathbf{d}_n = (\mathbf{d}_{n1}, \mathbf{d}_{n2})^T$ is a vector of dimension 6×1 partitioned in the submatrices $\mathbf{d}_{ni} = (u_{ni}, v_{ni}, \theta_{ni})^T$ of dimension 3×1 with $(i = 1, 2)$ and

$$\mathbf{a}(\xi) = [\mathbf{a}_1(\xi), \mathbf{a}_2(\xi)], \quad \mathbf{a}_i(\xi) = [\sin {}^1\alpha N_i^1, \cos {}^1\alpha N_{2i-1}^3, \cos {}^1\alpha N_{2i}^3]$$

$$\mathbf{b}(\xi) = [\mathbf{b}_1(\xi), \mathbf{b}_2(\xi)], \quad \mathbf{b}_i(\xi) = [0, \frac{dN_{2i-1}^3}{d\xi}, \frac{dN_{2i}^3}{d\xi}]$$

The components of the unbalanced resultant total pressure $\Delta p_h(\xi) = {}^2p_h(\xi) - {}^1p_h(\xi)$ at section ξ can be written as follows

$$ {}^2p_{hs} - {}^1p_{hs} = -\sin{}^1\theta_n \left[\mathbf{a}(\xi)\frac{\partial^1 p_h}{\partial y_c} + \mathbf{b}(\xi)\frac{\partial^1 p_h}{\partial \theta} \right] \mathbf{d}_n - {}^1p_h \cos{}^1\theta_n \mathbf{b}(\xi)\mathbf{d}_n \tag{42} $$

$$ {}^2p_{hn} - {}^1p_{hn} = \cos{}^1\theta_n \left[\mathbf{a}(\xi)\frac{\partial^1 p_h}{\partial y_c} + \mathbf{b}(\xi)\frac{\partial^1 p_h}{\partial \theta} \right] \mathbf{d}_n - {}^1p_h \sin{}^1\theta_n \mathbf{b}(\xi)\mathbf{d}_n \tag{43} $$

These components unbalanced forces $\Delta p_{hs}(\xi) = {}^2p_{hs}(\xi) - {}^1p_{hs}(\xi)$ and $\Delta p_{hn}(\xi) = {}^2p_{hn}(\xi) - {}^1p_{hn}(\xi)$ are replaced by the equivalent nodal forces p_{hsi}, p_{hni} and p_{hmi} at nodes i, $(i = 1, 2)$ of the pipeline element, that are referred to the local axes and their values are computed according to the expressions (39), (38) and (40). The final results are then[1]

$$ p_{hsi} = {}^1L \int_0^1 N_i^1 \Delta p_{hs}(\xi) d\xi = \mathbf{k}_{L1j}\mathbf{d}_n + \mathbf{k}_{L2j}\mathbf{d}_n \quad \text{with} \quad i = 1, 2 \tag{44} $$

where $j = 1$ if $i = 1$; $\quad j = 4$ if $i = 2$

$$ p_{hni} = {}^1L \int_0^1 N_i^3 \Delta p_{hn}(\xi) d\xi = \mathbf{k}_{L1j}\mathbf{d}_n + \mathbf{k}_{L2j}\mathbf{d}_n \quad \text{with} \quad i = 1, 3 \tag{45} $$

where $j = 2$ if $i = 1$; $\quad j = 5$ if $i = 3$

$$ p_{hmi} = {}^1L \int_0^1 N_i^3 \Delta p_{hn}(\xi) d\xi = \mathbf{k}_{L1j}\mathbf{d}_n + \mathbf{k}_{L2j}\mathbf{d}_n \quad \text{with} \quad i = 2, 4 \tag{46} $$

where $j = 3$ if $i = 2$; $\quad j = 6$ if $i = 4$

(47)

The first row vectors $\mathbf{k}_{L1j}$ are coming from the integration of terms of the following type

$$ \mathbf{k}_{L1j} = \pm {}^1L \int_0^1 N_i^{(1,3)} \begin{pmatrix} \sin{}^1\theta_n \\ \cos{}^1\theta_n \end{pmatrix} \left[\mathbf{a}(\xi)\frac{\partial^1 p_h}{\partial y_c} + \mathbf{b}(\xi)\frac{\partial^1 p_h}{\partial \theta} \right] d\xi \tag{48} $$

and they correspond to the variation of the intensity of the follower forces. The second row vectors $\mathbf{k}_{L2j}$ are obtained as a consequences of the integration terms

$$ \mathbf{k}_{L2j} = \pm {}^1L \int_0^1 N_i^{(1,3)} {}^1p_h \begin{pmatrix} \sin{}^1\theta_n \\ \cos{}^1\theta_n \end{pmatrix} \mathbf{b}(\xi) d\xi \tag{49} $$

and in this case they correspond to the variation of the direction of the follower force.

The load stiffness matrices $\mathbf{k}_{L1}$ and $\mathbf{k}_{L2}$ relate the force vectors at nodes to the corresponding displacements and they can written

$$ \mathbf{p}_n = \mathbf{k}_{L1}\mathbf{d}_n + \mathbf{k}_{L2}\mathbf{d}_n = \mathbf{k}_L\mathbf{d}_n \tag{50} $$

[1] It is usual to distinguish between the load matrices of de dimension 6×6 the matrices $\mathbf{k}_{L1}$ generated by an increment of differential vertical displacement y_c and the matrices $\mathbf{k}_{L2}$ produced by un angle change θ of the section of application of the load pressure. The former load matrices $\mathbf{k}_{L1}$ and $\mathbf{k}_{L2}$ are partitioned in row matrices j, $\mathbf{k}_{L1j}$ and $\mathbf{k}_{L2j}$.

where

$$\mathbf{p}_n = \begin{bmatrix} \mathbf{p}_{n1} \\ \mathbf{p}_{n2} \end{bmatrix}, \mathbf{d}_n = \begin{bmatrix} \mathbf{d}_{n1} \\ \mathbf{d}_{n2} \end{bmatrix}, \mathbf{k}_{Lj} = \begin{bmatrix} \mathbf{k}_{Lj1} \\ \mathbf{k}_{Lj2} \\ \mathbf{k}_{Lj3} \\ \mathbf{k}_{Lj4} \\ \mathbf{k}_{Lj5} \\ \mathbf{k}_{Lj6} \end{bmatrix} \quad (j = 1, 2)$$

where la matriz $\mathbf{k}_L$ is partitioned as follows

$$\begin{bmatrix} \mathbf{p}_{n1} \\ \mathbf{p}_{n2} \end{bmatrix} = \begin{bmatrix} \mathbf{k}_{L11} & \mathbf{k}_{L12} \\ \mathbf{k}_{L21} & \mathbf{k}_{L22} \end{bmatrix} \begin{bmatrix} \mathbf{d}_{n1} \\ \mathbf{d}_{n2} \end{bmatrix}$$

Finally, the expressions of these matrices in general axes are modified by means of suitable axes transformations. In this way the following final expressions are found

$$\mathbf{P} = \mathbf{K}_L \mathbf{D}, \text{ i.e. } \begin{bmatrix} \mathbf{P}_1 \\ \mathbf{P}_2 \end{bmatrix} = \begin{bmatrix} \mathbf{K}_{L11} & \mathbf{K}_{L12} \\ \mathbf{K}_{L21} & \mathbf{K}_{L22} \end{bmatrix} \begin{bmatrix} \mathbf{D}_1 \\ \mathbf{D}_2 \end{bmatrix} \tag{51}$$

where

$$\mathbf{P}_i = (p_{xi}, p_{yi}, m_{zi})^T, \quad \mathbf{D}_i = (d_{xi}, d_{yi}, \theta_{zi})^T$$

These vectors are related to the former vectors expressed in local axes by the transformation formulae

$$\mathbf{P}_i = \mathbf{T}\mathbf{p}_{ni}, \quad \mathbf{D}_i = \mathbf{T}^T \mathbf{d}_{ni} \quad \mathbf{K}_{L\alpha\beta} = \mathbf{T}\mathbf{k}_{L\alpha\beta}\mathbf{T}^T$$

where

$$\mathbf{T} = \begin{bmatrix} \cos {}^1\alpha & -\sin {}^1\alpha & 0 \\ \sin {}^1\alpha & \cos {}^1\alpha & 0 \\ 0 & 0 & 1 \end{bmatrix}$$

¿From a computational point of view it is convenient to use the matrices as functions of the type $\mathbf{k}_L = \mathbf{k}_L(y_{c1}, y_{c2}, {}^1\alpha)$ and $\mathbf{p} = \mathbf{p}(y_{c1}, y_{c2}, {}^1\alpha)$.

4. Pressure resultante on the pipeline lids

Similarly to the section 2. the loads on the two extreme sections or lids of the pipeline are studied. En particular the force and moment resultants of the pressure distribution on each of these extreme sections are obtained.

The force resultant, p^{α}_{hL} and the moment m^{α}_{hL} of the pressure distribution acting at extreme sections represented in figure 5 at the center of gravity of the section, are computed as follows. For each lid of the pipeline ($\alpha = 0$ and $\alpha = 1$) i.e. according to section $x = 0$ and $x = L$ of the initial pipeline position respectively, the computation of these forces and moments, as well as their derivatives respect to to the ordinate $y_{cL\alpha}$ and to the inclination

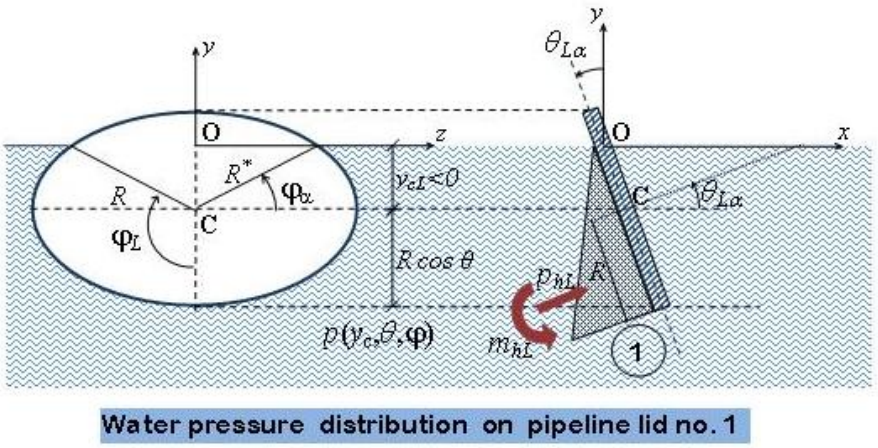

Figure 5: Pressure distribution on the end section of the pipeline

angle $\theta_{L\alpha}$ of the tube, are carried out. This inclination angle respect to the horizontal or slope at each tube end section is in general different to each end pipeline section α.

The following results for the force p^{α}_{hL} and the moment m^{α}_{hL} pressure resultants on the pipeline end section α:

Section in the air $\quad y_{cL\alpha} \geq R_{ext}\cos\theta_{L\alpha}$ (52)

$$p^{\alpha}_{hL} = 0$$

$$m^{\alpha}_{hL} = 0$$

Semi-submerged section $\quad R_{ext}\cos\theta_{L\alpha} \geq y_{cL\alpha} \geq -R_{ext}\cos\theta_{L\alpha}$ (53)

$$p^{\alpha}_{hL} = \varepsilon 2\gamma_w R^2_{ext}\left[\frac{y_{cL\alpha}}{2}\left(\varphi_\alpha + \sin\varphi_\alpha\cos\varphi_\alpha + \frac{\pi}{2}\right) - \frac{R_{ext}\cos^3\varphi_\alpha}{3}\right]$$

$$m^{\alpha}_{hL} = \varepsilon 2\gamma_w R^3_{ext}\left[-\frac{y_{cL\alpha}\cos^3\varphi_\alpha}{3} + \frac{R_{ext}}{16}(2\varphi_\alpha - \sin 2\varphi_\alpha\cos 2\varphi_\alpha + \pi)\right]$$

Submerged section $\quad y_{cL\alpha} \leq -R_{ext}\cos\theta_{L\alpha}$ (54)

$$p^{\alpha}_{hL} = \varepsilon\gamma_w\pi R^2_{ext}y_{cL\alpha}$$

$$m^{\alpha}_{hL} = \varepsilon\frac{1}{3}\gamma_w\pi R^4_{ext}$$

where

$$\sin\varphi_\alpha = -\frac{y_{cL\alpha}}{R_{ext}\cos\theta_{L\alpha}} \quad \text{and} \quad \varepsilon = (-1)^{\alpha} \tag{55}$$

The occurrence of small variations, v_0 and θ_0, of the depth $y_{cL\alpha}$ and rotation $\theta_{L\alpha}$ respectively, of section α, the increment of the resultant pressure force p^{α}_{hL} and its moment m^{α}_{hL}

are given by the formulae

$$\Delta p_{hL}^{\alpha} = \frac{\partial p_{hL}^{\alpha}}{\partial y_{cL\alpha}} v_0 + \frac{\partial p_{hL}^{\alpha}}{\partial \theta \alpha} \theta_0 \quad \text{and} \quad \Delta m_{hL}^{\alpha} = \frac{\partial m_{hL}^{\alpha}}{\partial y_{cL\alpha}} v_0 + \frac{\partial m_{hL}^{\alpha}}{\partial \theta \alpha} \theta_0 \tag{56}$$

The expressions of the derivatives $\frac{\partial p_{hL}^{\alpha}}{\partial y_{cL\alpha}}$, $\frac{\partial m_{hL}^{\alpha}}{\partial y_{cL\alpha}}$ de p_{hL}^{α} and m_{hL}^{α} respect to $y_{cL\alpha}$ are obtained as follows:

Section in the air $\quad y_{cL\alpha} \geq R_{ext} \cos\theta_{L\alpha}$ (57)

$$\frac{\partial p_{hL}^{\alpha}}{\partial y_{cL\alpha}} = 0$$

$$\frac{\partial m_{hL}^{\alpha}}{\partial y_{cL\alpha}} = 0$$

Semi-submerged section $\quad R_{ext} \cos\theta_{L\alpha} \geq y_{cL\alpha} \geq -R_{ext} \cos\theta_{L\alpha}$ (58)

$$\frac{\partial p_{hL}^{\alpha}}{\partial y_{cL\alpha}} = \varepsilon 2 \gamma_w R_{ext}^2 \left[\frac{1}{2} \left(\varphi_\alpha + \sin\varphi_\alpha \cos\varphi_\alpha + \frac{\pi}{2} \right) + (y_{hL\alpha} \cos^2\varphi_\alpha + R_{ext} \cos^2\varphi_\alpha \sin\varphi_\alpha) \frac{\partial \varphi_\alpha}{\partial y_{cL\alpha}} \right]$$

$$\frac{\partial m_{hL}^{\alpha}}{\partial y_{cL\alpha}} = \varepsilon 2 \gamma_w R_{ext}^3 \left[-\frac{\cos^3\varphi_\alpha}{3} + (y_{cL\alpha} \cos^2\varphi_\alpha \sin\varphi_\alpha + R_{ext} \sin^2\varphi_\alpha \cos^2\varphi_\alpha) \frac{\partial \varphi_\alpha}{\partial y_{cL\alpha}} \right]$$

Submerged section $\quad y_{cL\alpha} \leq -R_{ext} \cos\theta_{L\alpha}$ (59)

$$\frac{\partial p_{hL}^{\alpha}}{\partial y_{cL\alpha}} = \varepsilon \gamma_w \pi R_{ext}^2$$

$$\frac{\partial m_{hL}^{\alpha}}{\partial y_{cL\alpha}} = 0$$

where

$$\frac{\partial \varphi_\alpha}{\partial y_{cL\alpha}} = -\frac{1}{R_{ext} \cos\theta_{L\alpha}} \frac{1}{\sqrt{1 - \sin^2\varphi_\alpha}} \tag{60}$$

The derivatives $\frac{\partial p^{\alpha}_{hL}}{\partial \theta_{L\alpha}}$, $\frac{\partial m^{\alpha}_{hL}}{\partial \theta_{L\alpha}}$ de ∂p^{α}_{hL} and ∂m^{α}_{hL} respect to $\theta_{L\alpha}$ are respectively:

Section in the air $\quad y_{cL\alpha} \geq R_{ext}\cos\theta_{L\alpha}$ (61)

$$\frac{\partial p^{\alpha}_{hL}}{\partial \theta_{L\alpha}} = 0$$
$$\frac{\partial m^{\alpha}_{hL}}{\partial \theta_{L\alpha}} = 0$$

Semi-submerged section $\quad R_{ext}\cos\theta_{L\alpha} \geq y_{cL\alpha} \geq -R_{ext}\cos\theta_{L\alpha}$ (62)

$$\frac{\partial p^{\alpha}_{hL}}{\partial \theta_{L\alpha}} = \varepsilon 2\gamma_w R^2_{ext}\left[(y_{cL\alpha}\cos^2\varphi_\alpha + R_{ext}\cos^2\varphi_\alpha\sin\varphi_\alpha)\frac{\partial\varphi_\alpha}{\partial\theta_{L\alpha}}\right]$$
$$\frac{\partial m^{\alpha}_{hL}}{\partial \theta_{L\alpha}} = \varepsilon 2\gamma_w R^3_{ext}\left[(y_{cL\alpha}\cos^2\varphi_\alpha\sin\varphi_\alpha + R_{ext}\sin^2\varphi_\alpha\cos^2\varphi_\alpha)\frac{\partial\varphi_\alpha}{\partial\theta_{L\alpha}}\right]$$

Submerged section $\quad y_{cL\alpha} \leq -R_{ext}\cos\theta_{L\alpha}$ (63)

$$\frac{\partial p^{\alpha}_{hL}}{\partial \theta_{L\alpha}} = 0$$
$$\frac{\partial m^{\alpha}_{hL}}{\partial \theta_{L\alpha}} = 0$$

where

$$\frac{\partial\varphi_\alpha}{\partial\theta_{L\alpha}} = -\frac{y_{cL\alpha}}{R_{ext}\cos^2\theta_{L\alpha}}\sin\theta_{L\alpha} \tag{64}$$

The two groups of former expressions of the derivatives of the pressure follower forces on the lids of the pipeline represent two elastic springs attached to the pipeline extreme sections α. One of them elastically restrained the end section displacement and the another the end section rotation. From the computational point of view it is convenient to express the analysis in general coordinates by means the following transformation formulae:

$$\Delta p^{\alpha}_{hLx} = \Delta p^{\alpha}_{hL}\cos\theta_{L\alpha} = \left(\frac{\partial p^{\alpha}_{hL}}{\partial y_{cL\alpha}}v_0 + \frac{\partial p^{\alpha}_{hL}}{\partial\theta_{L\alpha}}\theta_0\right)\cos\theta_{L\alpha} \tag{65}$$

$$\Delta p^{\alpha}_{hLy} = \Delta p^{\alpha}_{hL}\sin\theta_{L\alpha} = \left(\frac{\partial p^{\alpha}_{hL}}{\partial y_{cL\alpha}}v_0 + \frac{\partial p^{\alpha}_{hL}}{\partial\theta_{L\alpha}}\theta_0\right)\sin\theta_{L\alpha} \tag{66}$$

$$\Delta m^{\alpha}_{hLz} = \Delta m^{\alpha}_{hL} = \frac{\partial m^{\alpha}_{hL}}{\partial y_{cL\alpha}}v_0 + \frac{\partial m^{\alpha}_{hL}}{\partial\theta\alpha}\theta_0 \tag{67}$$

These equations can be written in the compact form

$$\Delta\mathbf{p}^{\alpha}_{hL} = \mathbf{k}^{\alpha}_{hL}\mathbf{d}^{\alpha}_{hL} \quad \text{with} \quad \mathbf{k}^{\alpha}_{hL} = \begin{bmatrix} 0 & \frac{\partial p^{\alpha}_{hL}}{\partial y_{cL\alpha}}\cos\theta_{L\alpha} & \frac{\partial p^{\alpha}_{hL}}{\partial\theta_{L\alpha}}\cos\theta_{L\alpha} \\ 0 & \frac{\partial p^{\alpha}_{hL}}{\partial y_{cL\alpha}}\sin\theta_{L\alpha} & \frac{\partial p^{\alpha}_{hL}}{\partial\theta_{L\alpha}}\sin\theta_{L\alpha} \\ 0 & \frac{\partial m^{\alpha}_{hL}}{\partial y_{cL\alpha}} & \frac{\partial m^{\alpha}_{hL}}{\partial\theta\alpha} \end{bmatrix} \tag{68}$$

and where the force and displacement vector at pipeline end sections $\alpha = 0, 1$ are defined as follows:

$$\Delta \mathbf{p}_{hL}^{\alpha} = [\Delta p_{hLx}^{\alpha}, \Delta p_{hLy}^{\alpha}, \Delta m_{Lz}^{\alpha}]^T \quad \text{and} \quad \mathbf{d}_{hL}^{\alpha} = [d_x^{\alpha}, d_y^{\alpha}, \theta^{\alpha}]^T$$

Similarly the load vector acting at pipeline end section α is defined as

$$\mathbf{p}_{hL}^{\alpha} = [p_{hLx}^{\alpha}, p_{hLy}^{\alpha}, m_{Lx}^{\alpha}]^T$$

5. Stiffness matrix of an element

In addition to the the load stiffness matrices obtained in the previous section the nonlinear stiffness matrix of each beam element of pipeline should be computed. With this objective the incremental equilibrium equations between configurations C_1 and C_2 are formulated and they are discretized by means of the FE method. The obtained results assuming all loads, $\mathbf{F}_i = (F_{xi}, F_{yi}, M_{zi})^T$, $(i = 1, 2)$, are applied at end nodes i, $i = 1, 2$, can be written according to [3], [1], en forma matricial como sigue:

$$\left[{}^1\mathbf{k}_l + {}^1\mathbf{k}_g\right] \mathbf{d} = {}^2\mathbf{f} - {}^1\mathbf{f} \tag{69}$$

with $\mathbf{k}_l$ and $\mathbf{k}_g$ the linear and the geometric stiffness matrix of a 2-D beam element respectively. The displacement increments produced by the change of configuration from C_1 to C_2 caused by the the increasing of the external loads, ${}^2\mathbf{f} - {}^1\mathbf{f}$, are collected in the vector

$$\mathbf{d} = \begin{bmatrix} \mathbf{d}_1 \\ \mathbf{d}_2 \end{bmatrix} \quad \text{and the forces are} \quad {}^k\mathbf{f} = \begin{bmatrix} {}^k\mathbf{f}_1 \\ {}^k\mathbf{f}_2 \end{bmatrix} \tag{70}$$

with $\mathbf{d}_i = (d_{xi}, d_{yi}, \theta_i)$ the displacement increments of node i $(i = 1, 2)$. The applied external loads are ${}^k\mathbf{f}_i = ({}^kF_{xi}, {}^kF_{yi}, {}^kM_{zi})^T$ with $k = 1, 2$ and $i = 1, 2$

The expression of the linear stiffness matrix is:

$$\mathbf{k}_l = \begin{bmatrix} \frac{E\Omega}{L} & 0 & 0 & -\frac{E\Omega}{L} & 0 & 0 \\ 0 & 12\frac{EI_z}{L^3} & 6\frac{EI_z}{L^2} & 0 & -12\frac{EI_z}{L^3} & 6\frac{EI_z}{L^2} \\ 0 & 6\frac{EI_z}{L^2} & 4\frac{EI_z}{L} & 0 & -6\frac{EI_z}{L^2} & 2\frac{EI_z}{L} \\ -\frac{E\Omega}{L} & 0 & 0 & \frac{E\Omega}{L} & 0 & 0 \\ 0 & -12\frac{EI_z}{L^3} & -6\frac{EI_z}{L^2} & 0 & 12\frac{EI_z}{L^3} & -6\frac{EI_z}{L^2} \\ 0 & 6\frac{EI_z}{L^2} & 2\frac{EI_z}{L} & 0 & -6\frac{EI_z}{L^2} & 4\frac{EI_z}{L} \end{bmatrix} \tag{71}$$

with Ω the area of the resistant cross-section of the beam and I_z is the moment of inertial of the cross-section about the axis z.

The geometric stiffness matrix is

$$\mathbf{k}_g = \begin{bmatrix} \mathbf{k}_{g11} & \mathbf{k}_{g12} \\ \mathbf{k}_{g21} & \mathbf{k}_{g22} \end{bmatrix} \tag{72}$$

where

$$\mathbf{k}_{g11} = \begin{bmatrix} \frac{F_{x2}}{L} & 0 & -\frac{M_{z1}}{L} \\ 0 & \frac{6}{5}\frac{F_{x2}\left(\Omega L^2+10I_z\right)}{\Omega L^3} & \frac{1}{10}\frac{F_{x2}\left(\Omega L^2+60I_z\right)}{\Omega L^2} \\ -\frac{M_{z1}}{L} & \frac{1}{10}\frac{F_{x2}\left(\Omega L^2+60I_z\right)}{\Omega L^2} & \frac{2}{15}\frac{F_{x2}\left(\Omega L^2+30I_z\right)}{\Omega L} \end{bmatrix} \tag{73}$$

$$\mathbf{k}_{g12} = \begin{bmatrix} -\frac{F_{x2}}{L} & 0 & -\frac{M_{z2}}{L} \\ 0 & -\frac{6}{5}\frac{F_{x2}\left(\Omega L^2+10I_z\right)}{\Omega L^3} & \frac{1}{10}\frac{F_{x2}\left(\Omega L^2+60I_z\right)}{\Omega L^2} \\ \frac{M_{z1}}{L} & -\frac{1}{10}\frac{F_{x2}\left(\Omega L^2+60I_z\right)}{\Omega L^2} & \frac{1}{30}\frac{F_{x2}\left(-\Omega L^2+60I_z\right)}{\Omega L} \end{bmatrix} = \mathbf{k}_{g21}^T \tag{74}$$

$$\mathbf{k}_{g22} = \begin{bmatrix} \frac{F_{x2}}{L} & 0 & \frac{M_{z2}}{L} \\ 0 & \frac{6}{5}\frac{F_{x2}\left(\Omega L^2+10I_z\right)}{\Omega L^3} & -\frac{1}{10}\frac{F_{x2}\left(\Omega L^2+60I_z\right)}{\Omega L^2} \\ \frac{M_{z2}}{L} & -\frac{1}{10}\frac{F_{x2}\left(\Omega L^2+60I_z\right)}{\Omega L^2} & \frac{2}{15}\frac{F_{x2}\left(\Omega L^2+30I_z\right)}{\Omega L} \end{bmatrix} \tag{75}$$

It is noticed that the former stiffness matrices, $\mathbf{k}_l$ and $\mathbf{k}_g$, are symmetric as correspond to a conservative (adjoint) problem.

In the former results is was assumed that the only loads applied on the element are the ones acting at its end nodes, i.e. $\mathbf{F}_i = (F_{xi}, F_{yi}, M_{zi})^T$, $(i = 1, 2)$. Then the stress-resultants at section ξ of the element produced by the loads acting directly on the element span (weight and hydrostatic pressure) must be added the stress-resultants corresponding to the loads $\mathbf{F}_i$:

$$F_x = F_{x1} = -F_{x2},\ F_y = -\frac{M_{z1} + M_{z2}}{L},\ M_z = -M_{z1}(1-\xi) + M_{z2}\xi \tag{76}$$

The equations (76) represent the stress-resultants at section ξ as function of the reactions of the beam element at its end nodes. They have been obtained using the static equilibrium of the beam element.

6. Incremental equilibrium equations of the pipeline

The initial configuration C_0 of the pipeline without initial stresses corresponds to the tube subjected only to the uniforme distributed loads of weight p and uplift hydrostatic pressure $p_h(y_c, \theta)$. The equilibrium position corresponds to the pipeline floating horizontally, $\theta = 0$, at depth y_c defined as the solution of the equation $p_h(y_c, \theta = 0) = p$. The loads due to the horizontal pressure on lids $\mathbf{p}_{hL}$ and to the weight $\mathbf{P}_L$ of the pipeline extreme section, i.e. to the lids, are monotonically introduced from this equilibrium position by means a factor λ varying from 0 up to 1.

In a load step it it is assumed known at configuration C_1 all the applied loads, the equivalent nodal forces at element nodes i of each element j, the variation of deflections and rotations along the pipeline span and the stress-resultants as well, i.e. the following functions

are known

$$\text{Loading:} \quad p, \quad {}^1p_{hi}(\xi)\,(i=1,2,\ldots,N), \quad \lambda P_{L\alpha}\,(\alpha=0,1), \quad \lambda {}^1\mathbf{p}^{\alpha}_{hL} \tag{77}$$

$$\text{Equivalent nodal forces:} \quad {}^1\mathbf{F}^{j}_{i},\ (i=1,2)\,(j=1,2,\ldots,N) \tag{78}$$

$$\text{deflections and rotations:} \quad {}^1x^{j}_{i},\ {}^1y^{j}_{i},\ {}^1\theta^{j}_{i},\ (i=1,2)\,(j=1,2,\ldots,N) \tag{79}$$

$$\text{Stres-resultants:} \quad {}^1F^{j}_{x}(\xi),\ {}^1F^{j}_{y}(\xi),\ {}^1M^{j}_{z}(\xi),\ (j=1,2,\ldots,N) \tag{80}$$

If the following load increments, $d\lambda P_{L\alpha}$ and $d\lambda {}^1\mathbf{p}^{\alpha}_{hL}$, are introduced on the end sections of the pipeline, $\alpha = 0, 1$, then the pipeline experiments the displacements $\mathbf{d}^{j}_{i}$ at nodes $i = 1, 2$ of all elements j. The matrix equation of equilibrium can be written

$$\mathbf{KD} = \mathbf{P} \tag{81}$$

where

$$\mathbf{K} = \sum_{\alpha}[\mathbf{k}^{\alpha}_{l} + \mathbf{k}^{\alpha}_{g} - \mathbf{k}^{\alpha}_{L1} - \mathbf{k}^{\alpha}_{L2}]\mathbf{D} + \lambda \sum_{\alpha=0,1} \mathbf{k}^{\alpha}_{hL}\mathbf{d}^{\alpha}_{hL} = d\lambda \sum_{\alpha=0,1} [\mathbf{p}_{hL} + \mathbf{P}_{L\alpha}]$$

and $\mathbf{P}_{L\alpha} = P_{L\alpha}[0, -1, 0]^T$ is the vector of gravitational loads concentrated at section α. The summations correspond to boolean sums or assembly of all element matrices and vectors of the structural elements. In this way the whole global structure matrices and vector can be built.

The solution of the system of simultaneous linear equations represented by the matrix equation (81) can be carried our by a direct numerical solution method and the displacement vector **D** expressed in global exes is obtained. It is possible to increase the solution accuracy by iterative procedure within the current load step.

Once the displacements are know in the load step it is possible to define all the variables of interest for the configuration C_2. These variables should be changed by transforming them to the new coordinate system defined by the achieved configuration C_2, i.e. a coordinate transformation should be performed in order to change the already known configuration C_2 into the new configuration C_1 for the new load step.

7. Examples

7..1. Symmetric pipeline

In order to illustrate the described analysis a simple example will be presented. The following data of a symmetric pipeline, i.e. with equal lids will be considered: *Length*: 18 m, *Inner radius*: 0,945 m, *External radius*: 1 m
Young modulus: 2×10^5 kN/m2, *Specific weight*: 77 kN/m3, *Water specific weight*: 10,29 kN/m3
The two pipeline lids are equal with thickness 6 cm and weight 14,516 kN each. The total tube weight, lids no included, is: 465,85 kN
The pipeline is discretized in 48 elements.

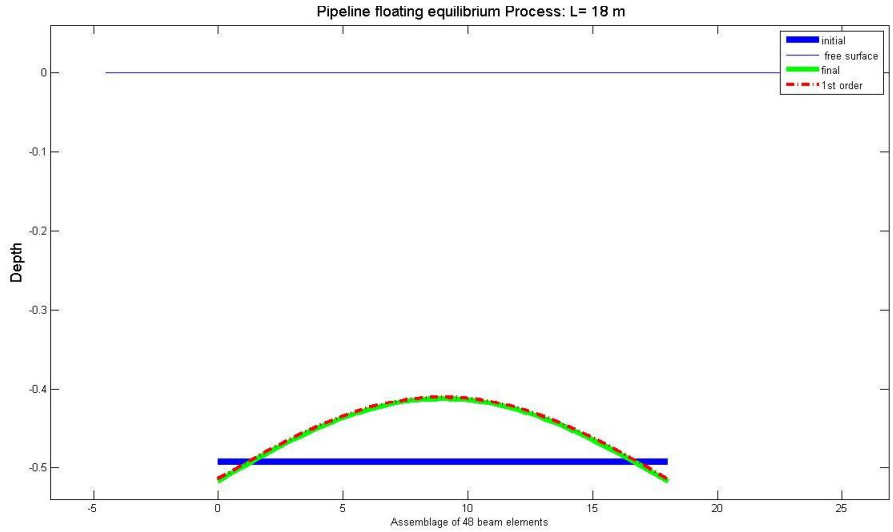

Figure 6: Symmetric pipeline

In figure 6 the deformed pipeline obtained by a linear analysis is shown. Also the deformed pipeline found according to a more elaborated analysis, namely, a nonlinear analysis using an incremental and iterative procedure is presented in the figure. It can be observed that the first order analysis produces larger displacements than the nonlinear analysis.

The initial equilibrated position of the tube (tube weight without lids and uplift Archimedes pressure) is reached for a axis pipeline position of -0,4929 meters.

7..2. Nonsymmetric pipeline

The tube used in this example corresponds to the previous tube but with different lid thicknesses. One lid has 6 cm of thickness and the other 9 cm. The results are shown in figure 7

8. Conclusions

Analysis of this type of pipeline of elements represent an interesting example of the application of nonlinear large displacement methodology. A better understanding of the structural behavior of these structures can permit to obtain improved models for the laying process of submarine emissaries.

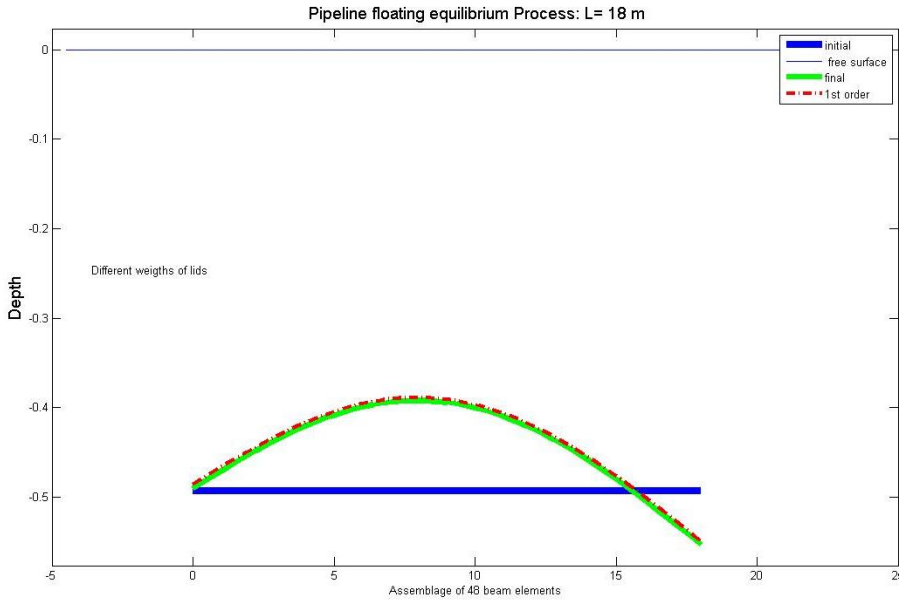

Figure 7: Nonsymmetric pipeline

9. Acknowledgments

The financial support for this work provided by the *Dirección General de Investigación* of the Spanish Ministry of Education and Science under the research contract DPI2005-09203-02 is grateful recognized by the authors.

References

[1] García-Palacios, J. and Samartín, A. and Negro, V. A nonlinear analysis of laying a floating pipeline on the seabed. *Engineering Structures*, 31(5):1120–1131, 2009.

[2] Schweizerhof, K. and Ramm, E. Displacement dependent pressure loads in nonlinear finite element analisys. *Computer and Structures*, 18(1):1099–1114, 1984.

[3] Yang, Y.B. and Kuo, S.R. *Theory and Analysis of Nonlinear Frame Structures*. Prentice Hall Inc., Upper Saddle River, NJ 07456, 2nd edition, 1994.